Chemical Physics Letters 564 (2013) 60–64

Contents lists available at SciVerse ScienceDirect

Chemical Physics Letters

journal homepage: www.elsevier.com/locate/cplett

Computational and experimental studies of the interaction between single-walled carbon nanotubes and folic acid

John J. Castillo [a,b], Ciro E. Rozo [c], Jaime Castillo-León [d,*], Tomas Rindzevicius [d], Winnie E. Svendsen [d], Noemi Rozlosnik [d], Anja Boisen [d], Fernando Martínez [a]

[a] Centro de Investigaciones en Catálisis, Universidad Industrial de Santander, Sede Guatiguará UIS Km 2 vía Refugio, Piedecuesta, Colombia
[b] Grupo de Investigación en Ciencias Químicas y Tecnologías Sostenibles, Facultad de Ciencias Físicas, Exactas y Naturales, Universidad de Santander, Campus Lagos del Cacique, Bucaramanga, Colombia
[c] Grupo de Investigaciones Ambientales para el Desarrollo Sostenible, Facultad de Química Ambiental, Universidad Santo Tomas, Floridablanca, Colombia
[d] Department of Micro and Nanotechnology, Technical University of Denmark, 2800 Lyngby, Denmark

ARTICLE INFO

Article history:
Received 2 January 2013
In final form 6 February 2013
Available online 18 February 2013

ABSTRACT

This Letter involved the preparation of a conjugate between single-walled carbon nanotubes and folic acid that was obtained without covalent chemical functionalization using a simple 'one pot' synthesis method. Subsequently, the conjugate was investigated by a computational hybrid method: our own N-layered Integrated Molecular Orbital and Molecular Mechanics (B3LYP(6–31G(d):UFF)). The results confirmed that the interaction occurred via hydrogen bonding between protons of the glutamic moiety from folic acid and π electrons from the carbon nanotubes. The single-walled carbon nanotube-folic acid conjugate presented herein is believed to lead the way to new potential applications as carbon nanotube-based drug delivery systems.

1. Introduction

Carbon nanotubes (CNTs) were discovered by Ijima in 1991 [1] and are characterized by the fact that they form a structure of thin layers of rolled benzene rings forming a cylindrical tube. CNTs belong to the family of fullerenes, the third allotropic form of carbon, after graphite and diamond [2]. According to their structure, CNTs are classified as single-walled and multi-walled carbon nanotubes (SWCNTs and MWCNTs, respectively). The former have been considered as one of the most promising nanostructures in the field of biomedicine. SWCNTs can potentially be used for biomedical applications ranging from biosensor technologies to drug delivery systems [3–5].

Recently the functionalization of SWCNTs with folic acid (FA) has been devoted much attention due to the importance of such conjugates as vectors in drug delivery systems [6,7]. FA is an attractive ligand that is useful for targeting cell membranes and enhancing CNT endocytosis by the folate receptor [8,9]. FA receptors can be direct targets for drug delivery and disease detection [10], which explains the diversity of strategies that folate conjugation can be utilized for.

Conventionally, SWCNTs–FA conjugates have been characterized by UV–Vis (ultraviolet–visible spectroscopy), NIR (near-infrared) spectroscopy [6], NMR (nuclear magnetic resonance) spectroscopy [11], AFM (atomic force microscopy) and TEM (transmission electronic microscopy), but they have yet to be investigated with computational methods. However, various studies have been performed using CNTs functionalized with different biomolecules [11–13]. Riahi et al. reported a computational study on the interaction between histidine and SWCNTs [14]. Recently, the adsorption of a variety of amino acids on armchair SWCNTs has been explored using calculations based on the density functional theory (DFT) [15]. In a similar investigation, Lemli et al. [16] studied the noncovalent interaction between aniline and CNTs, and UV–Vis spectra was used to further demonstrate the attachment of aniline to the SWCNTs.

It is important to be able to predict the interaction between FA and carbon nanotubes with changes in electronic structure in order to determine the nature of biological-nanotube interactions, and this knowledge is also critical for understanding their biological activity as well as the potential part they can play in nanostructure fabrication and carbon nanotube-based drug delivery systems.

This Letter presents the results of quantum chemical calculations on the interaction between one molecule of FA and a (5,5) armchair SWCNT. Raman and fluorescence spectroscopies were employed to characterize and to experimentally prove the attachment of FA to the surface of SWCNT. Finally, atomic force microscopy (AFM) revealed that the SWCNTs were indeed coated by FA. The results of these combined computational and experimental studies will open up possibilities for the development of new drug delivery systems for cancer therapies.

* Corresponding author.
E-mail address: jaic@nanotech.dtu.dk (J. Castillo-León).

0009-2614/$ - see front matter © 2013 Elsevier B.V. All rights reserved.
http://dx.doi.org/10.1016/j.cplett.2013.02.014

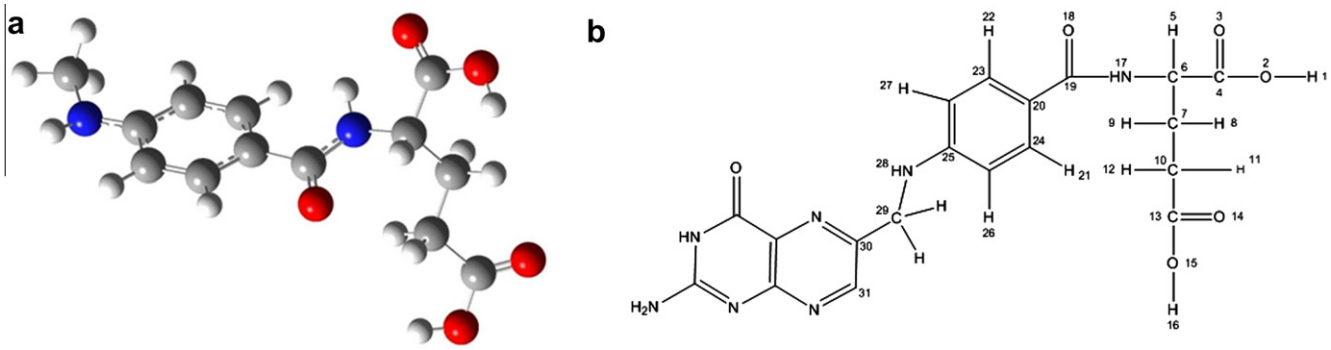

Figure 1. (a) Optimized geometry of the FA structure. (b) Chemical structure of FA.

2. Methods

2.1. Computational methods

The structures of FA and SWCNT were optimized with a hybrid method: our own N-layered Integrated Molecular Orbital (ONIOM) (B3LYP(6–31G(d):UFF)) [17]. In our calculations, an armchair (5,5) SWCNT comprising 110 carbon atoms and end-terminated with 10 hydrogen atoms (Figure S1) interacting with the FA structure was taken as the model system. The C–C bond in the SWCNT was 1.42 Å, which corresponds to a C=C bond with a sp^2 hybridization. The bond length used in this Letter was consistent with many earlier computational studies of SWCNTs [18,19].

The interaction of the SWCNTs with FA was determined by the density functional theory (DFT) [20] framework using the B3LYP [21] functional in conjunction with the 6-31G(d) basis set. All calculations were carried out using the Gaussian 09 suite of programs [22].

2.2. Experimental methods

SWCNTs with diameters ranging from 0.2 to 2 nm and lengths between 500 and 2000 nm were purchased from Unydim, California (USA). FA was obtained from the Sigma–Aldrich Corp. These and all other chemicals used in this Letter were of analytical grade.

5 mg of SWCNTs were ultrasonicated (Processor cpx 130PB Cole Parmer) for 15 min in 5 mL of a 5-mM aqueous solution of FA. The FA powder (0.011 g) had been mixed beforehand with water (5 mL), to which was added 10 μL of NaOH (1 M) due to the poor solubility of FA, and magnetically stirred until a yellow-to-clear transition was observed. The dispersion of SWCNT–FA was centrifuged at 12 000 rpm for 20 min. The supernatant was collected and carefully separated from the solid. After aggregation, the solution contained a large bundle of SWCNTs. The supernatant was washed with water several times to remove excess FA. Finally, the SWCNT–FA solution was stored at 4 °C.

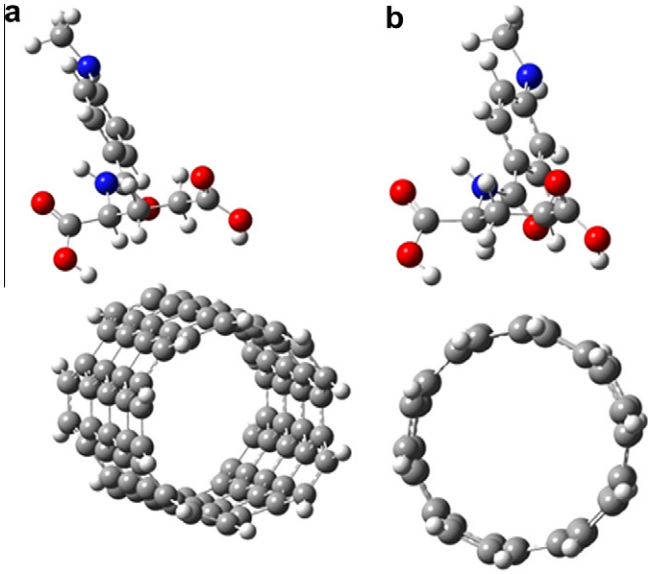

Figure 2. Full optimized structures of the SWCNT–FA conjugate; (a) diagonal view and (b) front view.

The fluorescence emission from SWCNTs-FA solutions was recorded using a standard Perkin Elmer LS-55 luminescence spectrophotometer with an excitation wavelength of 364 nm. Raman experiments were performed using a Thermo Scientific DXR Raman Microscope. An optical microscope was coupled to a single grating spectrometer with 5 cm^{-1} FWHM spectral resolution and ±2 wavenumber accuracy. A frequency-stabilized single diode laser was operated at 780 nm. Raman spectra were recorded using a 50× long working distance objective, 5 mW laser power and 10s signal accumulation times. All atomic force microscopy (AFM) images were recorded using an XE-150 Premier cross-functional AFM

Table 1
Comparison of internuclear distances of folic acid.

C_i–H_j Bond	Internuclear distance (Å)	Internuclear distance[a] (Å)
C23–H22	2.13	2.13
C20-H29	2.15	2.15
C17–H18	2.08	2.05
C11–H12/16	2.18(2.17)	2.17(2.16)
C13/15–H13/15	1.08	1.08
C14–H13/15	2.18(2.18)	2.16(2.14)

[a] Bonechi et al.

Table 2
Dihedral angle for free folic acid and folic acid interacting with carbon nanotubes.

Dihedral angle	Free FA (°)	FA–SWCNT (°)
C13–C10–C7–C6	175.8	183.0
C6–N17–C19–C20	187.7	169.3
C4–C6–N17–C19	282.4	225.2
C4–C6–C7–C10	66.4	177.7
C7–C6–N17–C19	157.7	102.8
N17–C6–C4–O2	62.6	167.2
C7–C10–C13–O15	180.1	130.1
C10–C13–O15–H16	180.4	355.2
H5–C6–C7–C10	38.6	343.2

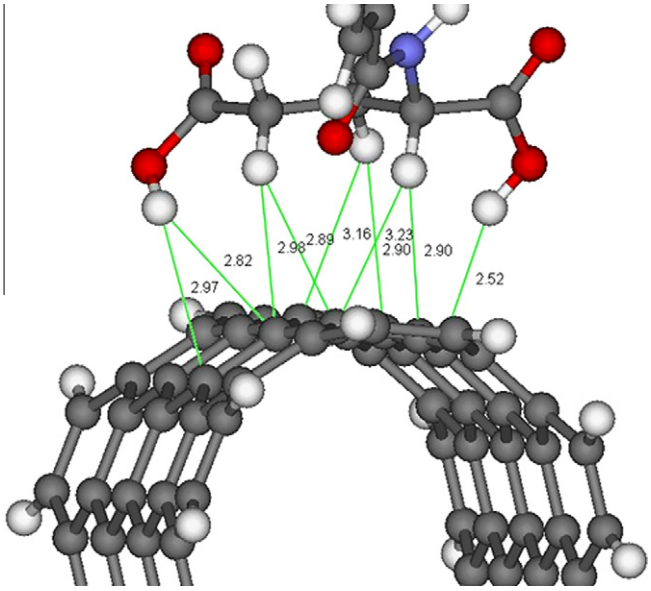

Figure 3. Full optimized structures of the GLU moiety from FA interacting with the surface of SWCNT.

(Park Systems, Korea) with a PPP-NVHR AFM probe (Nanosensors, Switzerland).

3. Results and discussion

The optimized structure of the free FA is depicted in Figure 1. According to the figure, the glutamic acid (GLU) and p-aminobenzoic moieties (PABA) were in the same molecular plane. The GLU γ moiety had a dihedral angle of 175.8° (C13–C10–C7–C6) and the dihedral angle from the union between GLU and PABA moieties was 187.7° (C6–N17–C19–C20). The GLU α moiety, on the other hand, was out of the plane with a dihedral angle of 282.4° (C4–C6–N17–C19).

Table 3
Peak positions of the D- and G-bands for SWCNT and SWCNT–FA dispersions as well as D/G ratios.

Sample	Raman shift (cm^{-1})		Intensity ratio D/G
	D	G	
SWCNT	1325	1580	0.186
SWCNT–FA	1328	1587	0.217

Furthermore the pteridine ring (PT) was perpendicular to the PABA moiety with a dihedral angle of 301.6° (C31–C30–C29–N28), and the torsion angle between PT and PABA was planar (175.3° (C30–C29–N28–C25)). Although these values have not been reported in the literature, Bonechi et al. [23] have published the interatomic distances (C_i–H_j) of FA, which were in concordance with the values obtained in this Letter. Table 1 shows a comparison between the interatomic distances of FA from the literature and the distances obtained here.

In order to reduce the complexity of the system and the analysis time, the computational simulation for the interaction between SWCNT and FA included only the GLU and PABA moieties. On the other hand, this approximation was considered since the PT ring from FA was involved in the interaction with folate receptors (FR) from the membrane cell [24]. For this reason, the interaction with the SWCNTs could be carried out only with the GLU moiety. Figure 2 shows the optimized structure of the FA interacting with the SWCNTs.

Geometrical parameters such as bond lengths and bond angles of the SWCNT interacting with FA remained almost unaltered. The C–C bond length was found to be 1.42 Å which was consistent with previous observations [18]. We believe that this could be due to the weak interactions between FA and the SWCNTs. On the other hand, the FA structure that was bound to the SWCNTs showed remarkable differences in the bond angles and bond distances from

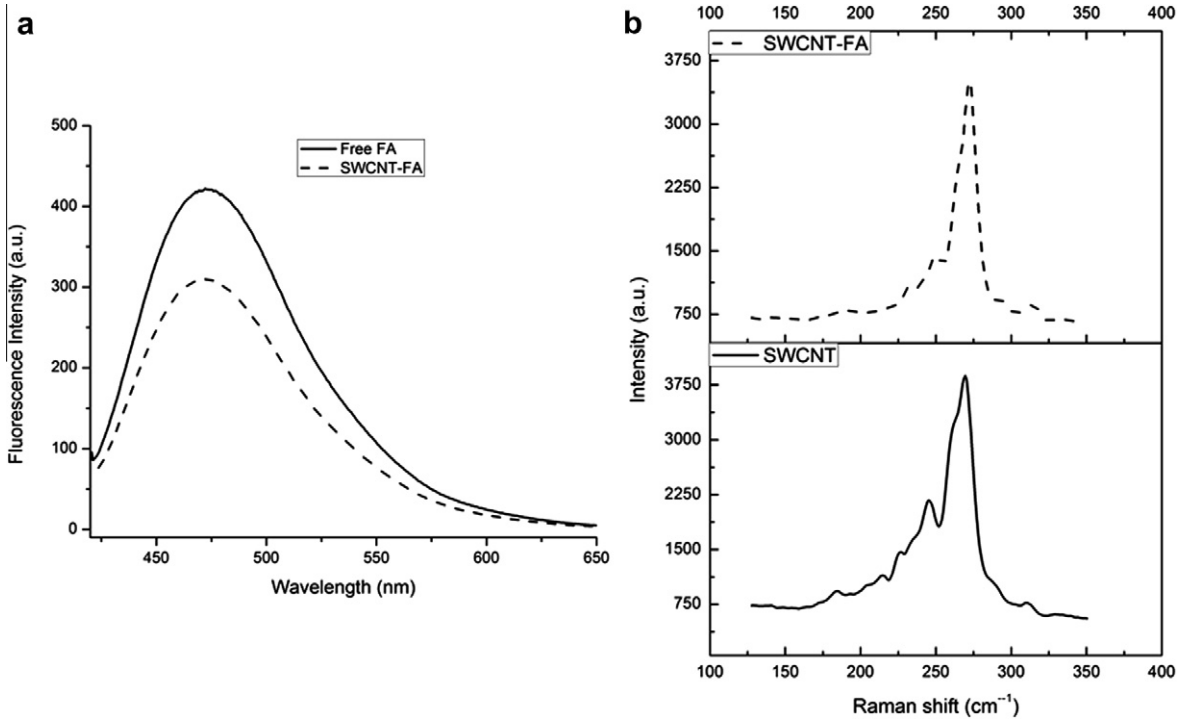

Figure 4. (a) Fluorescence spectra of free FA (solid line) and conjugated FA (dashed line) and (b) radial breathing modes (RBM) of non-functionalized SWCNTs (solid line) and FA-functionalized SWCNTs (dashed line).

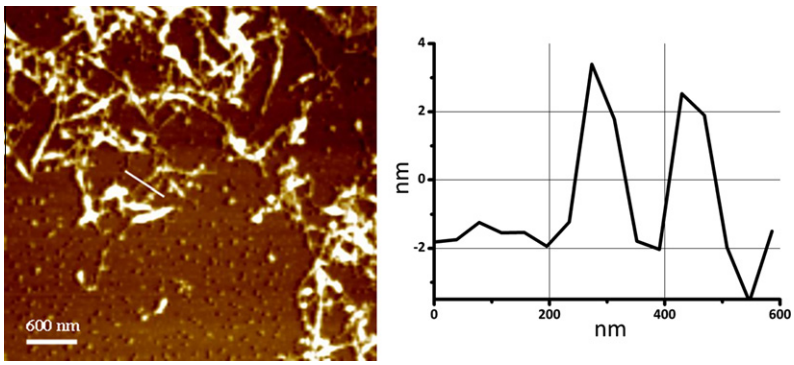

Figure 5. Topographic AFM micrograph of FA conjugated to SWCNT on a silicon susbstrate using imaging in non-contact mode.

the GLU moiety compared with free FA. Table 2 presents a comparison between the dihedral angle from the free and conjugated FA.

According to Table 2, there were remarkable differences with regard to the dihedral angle between free and conjugated FA. An example is the contrast between the angle formed by (N17–C6–C4–O2) from GLU and free FA (62.6°) as opposed to its counterpart for the FA SWCNT conjugate (167.2°). The structure of free FA enabled the formation of a hydrogen bond between O2 and O14 with a bond distance of 1.73 Å. This interaction was broken when FA was conjugated to the structure of carbon nanotube (5.45 Å); the proton was oriented in a favorable way for the interaction with the nanotube.

Hydrogen bonds occur when a donor atom donates its covalently bonded hydrogen atom to an electronegative acceptor atom [25]. Donor–acceptor distances of 2.2–2.5 Å as strong and covalent; 2.5–3.2 Å as moderate, mostly covalent; and 3.2–4.0 Å as weak electrostatic [25,26]. Figure 3 shows the distances between GLU moieties from FA and SWCNTs. According to Jeffrey and the results obtained in this Letter, the connection between FA and SWCNT was governed by weak interactions such as hydrogen bonds. This hydrogen interaction can be categorized as moderate in strength.

Experimental evidences were further performed to prove the weak interaction between FA and the carbon nanotubes. A comparison between the FA and SWCNT–FA fluorescence emission spectra is presented in Figure 4a. The fluorescence quenching by SWCNTs was observed as a decrease in the fluorescence intensity of free FA. This feature agreed well with the results previously presented [27].

Raman spectroscopy has been extensively utilized to study the vibrational modes and overtones of carbon nanotubes [28]. In particular, vibrational spectra can provide useful information when exploring the functionalization of SWCNTs. Figure 4b shows the evolution of the RBM of the nonfunctionalized and FA-coated SWCNTs. The intensity of the RBM at 270 cm^{-1}, also known as the roping peak [28], decreased after functionalization with FA. The intensity drop of the roping peak was evidence of a good dispersion [29], and the result verified the dual role of FA in the dispersion and functionalization of the SWCNTs. This can be further explained as a result of a low irregular distribution of sp^3 sites due to the noncovalent functionalization that decreased the intensity of the so-called van Hove singularities [30].

In addition to RBM, the disorder-induced D-band and the related G-band can be used to monitor the coating of the SWCNTs through weak interactions [31]. The I_D/I_G intensity ratios for the SWCNTs and the FA–SWCNT are shown in Table 3, and were found to be 0.186 and 0.217, respectively. These relatively small variations of the I_D/I_G ratios can be interpreted as an indication of a weak interaction character between FA and the carbon nanotubes. Covalent functionalizations, on the other hand, produce significantly larger defects on the surface of the SWCNTs [31].

Finally we determined the length and diameters of the FA-functionalized SWCNTs. Figure 5 shows a topographical 3×3 μm image of the SWCNT–FA conjugate. The protrusions with a size of 4 nm observed on the SWCNTs indicate the presence of FA around the carbon nanostructure (originally SWCNT have a diameter size ranging from 0.2 to 2 nm, see Section 2.2).

Thus, thanks to computational and experimental studies, we have provided strong evidence of the bonding between FA and SWCNTs through weak interactions such as hydrogen bonds.

4. Conclusions

This is the first report of the interactions between FA with carbon nanotubes as determined by computational tools. Complementary experimental studies showed the FA was coated on SWCNTs thanks to weak and noncovalent interactions such as hydrogen bonds. The SWCNT–FA conjugate analyzed here by computational and experimental techniques could be the first step toward an understanding of the interaction between FA and carbon nanotubes for future applications in drug delivery systems based on carbon nanostructures.

Acknowledgments

The Colombian Administrative Department of Science, Technology and Innovation, COLCIENCIAS, (Project 110245921468) and the Danish Agency for Science Technology and Innovation (FTP 271-08-0968) are gratefully acknowledged for financial support.

Appendix A. Supplementary data

Supplementary data associated with this article can be found, in the online version, at http://dx.doi.org/10.1016/j.cplett.2013.02.014.

References

[1] S. Iijima, Nature 354 (1991) 56.
[2] D. Tasis, A. Bianco, M. Prato, Chem. Rev. 106 (2006) 1105.
[3] A. Bhirde, J. Gavard, G. Zhang, A. Sousa, A. Masedunskas, ACS Nano 3 (2009) 307.
[4] M. Adeli, M. Ashiri, R. Kabiri, M. Bavadi, Soft Matter 7 (2011) 4062.
[5] N. Sahoo, Y. Pan, M. Pal, M. Kakran, H. Cheng, Chem. Commun. 47 (2011) 5235.
[6] B. Kang, Y. Dai, S. Chang, D. Cheng, Y. Ding, Small 5 (2009) 1292.
[7] W. Xia, J. Med. Chem. 53 (2010) 6811.
[8] X. Yang, Z. Liu, Y. Ma, R. Yang, Y. Chen, J. Nano Res. 10 (2008) 815.
[9] X. Zhang, Q. Lu, Z. Fei, P. Dyson, Biomaterials 30 (2009) 815.
[10] J. Castillo, W.E. Svendsen, N. Rozlosnik, P. Escobar, F. Martínez, J. Castillo-León, Analyst 138 (2013) 1026.

[11] J. Castillo, M. Torres, D. Molina, W. Svendsen, J. Castillo-León, P. Escobar, F. Martínez, Carbon 50 (2012) 2691.
[12] S. Yoshimura, H. Maruyama, Y. Nakayama, K. Takeyasu, Biomacromolecules 12 (2011) 1200.
[13] S. Madani, O. Dissanayake, A. Tan, A. Seifalian, Int. J. Nanomed. 6 (2011) 2963.
[14] S. Riahi, M. Ganjali, P. Norouzi, Int. J. Electrochem. Sci. 5 (2010) 1612.
[15] T. Roman, H. Nakanishi, H. Kasai, Eur. Phys. J. D 38 (2006) 117.
[16] B. Peles-Lemli, A. Kelterer, W. Fabian, S. Kunsági-Máté, J. Phys. Chem. C 114 (2010) 5898.
[17] S. Dapprich, I. Komaromi, K. Byun, K. Morokuma, M. Frisch, J. Mol. Struct.: THEOCHEM 461 (1999) 1.
[18] N. Cordero, J. Alonso, J. Phys. Chem. C 114 (2010) 17249.
[19] T. Ng, K. Liew, Int. J. Hydrogen Energy 35 (2010) 4543.
[20] P. Hohenberg, W. Kohn, Phys. Rev. 136 (1964) B864.
[21] A. Becke, J. Chem. Phys. 98 (1993) 5648.
[22] M. Frisch, G. Trucks, H. Schlegel, G. Scuseria, M. Robb, J. Cheeseman, Gaussian 09, Revision B.01, Gaussian, Inc., Wallingford, CT, 2010.
[23] C. Bonechi, R. Lampariello, S. Martini, M. Picchi, M. Ricci, C. Rossi, Spectrochim. Acta, Part A 60 (2004) 1411.
[24] C. Muller, U. Hoffmann, P. Schubiger, R. Schibli, J. Organomet. Chem. 689 (2004) 4712.
[25] A. Jeffrey, An Introduction to Hydrogen Bonding, Oxford University Press, 1997.
[26] E. Martz, Help, Index & Glossary for Protein Explorer, 2004.
[27] E. Cho, W. Jo, Macromol. Rapid Commun. 29 (2008) 1798.
[28] B. Koh, X. Hou, W. Cheng, J. Phys. Chem. B 115 (2011) 2627.
[29] D. Yoon, C. Han, Y. Kim, S. Baik, Carbon 46 (2008) 1530.
[30] L. Carson, M. Stewart, A. Oki, G. Regisford, Z. Luo, V. Bakhmutov, Mater. Lett. 63 (2009) 617.
[31] D. Horn, C. Easley, V. Davis, J. Phys. Chem. C 116 (2012) 10341.